International Journal of Mass Spectrometry 285 (2009) 105–113

Contents lists available at ScienceDirect

International Journal of Mass Spectrometry

journal homepage: www.elsevier.com/locate/ijms

A bipolar rate equation model of MALDI primary and secondary ionization processes, with application to positive/negative analyte ion ratios and suppression effects

Richard Knochenmuss*

ARTICLE INFO

Article history:
Received 18 March 2009
Received in revised form 11 May 2009
Accepted 12 May 2009
Available online 22 May 2009

Keywords:
MALDI
Ionization mechanisms
Rate equation
Ion ratios

ABSTRACT

The rate equation model for MALDI ion formation and reaction [R. Knochenmuss, J. Mass Spectrom. 37 (2002) 867; R. Knochenmuss, Anal. Chem. 75 (2003) 2199], including both chemical and physical dynamic aspects of MALDI, is extended to explicitly include both positive and negative ions of matrix and analyte. The resulting positive/negative ratios of secondary analyte ions show that a recent static equilibrium approach is not adequate for quantitative analysis of MALDI experiments. In particular, the ion ratios remain close to unity whenever the reaction free energies are at least moderately favorable. This is the case for high and low analyte concentrations and also for a range of experimental conditions. The results are consistent with the available experimental data, and show once again that the dynamic aspects of MALDI cannot be neglected. In addition, the extent of matrix and analyte suppression effects is found to depend on reactions in the opposite polarity.

1. Introduction

Most mass spectrometers used with MALDI ion sources measure one polarity at a time, so there is little directly comparable data regarding the relative strengths of positive and negative ion signals from the same or identical samples. This topic is nevertheless of interest for understanding of MALDI ionization mechanisms, which, in turn, can aid in selection of the best matrix and polarity for a particular analyte. Also important when analyzing complex samples with MALDI are suppression effects, where one component of the sample reduces signal from another. Suppression is shown here to be dependent on reactions in both polarities.

A 2007 study [1] investigated positive/negative analyte ion ratios (PNAIR) for several combinations of peptide analytes and common matrixes, using two different mass spectrometer and detector systems, and included efforts to correct for relative sensitivities. All investigated PNAIR were roughly on the order of one, although the scatter was large. Since the free energies of reaction between matrix ions and analytes spanned a significant range, this was interpreted as being inconsistent with a postulated thermodynamic equilibrium model for ionic species in the expanding plume.

The analysis in that study did not include mass balance, even though it has long been known that either matrix primary ions or analyte may be limiting reagents for secondary ion–molecule reactions [2,3]. Inclusion of mass balance for each polarity showed that the data are not necessarily inconsistent with approach to local thermal equilibrium (LTE) [4]. Subsequent extension of the mass balance concept to include coupling of the polarities via neutral precursors found limiting cases which could be consistent with 2007 data, and others which are not [5].

Although it was noted in [4] that the issue is really "approach to local thermal equilibrium", the recent discussion has drifted away from "approach" and focused too much on "equilibrium". The reality is that the MALDI plume is both highly dynamic and does not reach true equilibrium. This is not a new concept, as noted in a 2006 review of MALDI ionization mechanisms [6] "complete relaxation and thermal equilibrium is never attained because the expansion becomes so dilute that reactions effectively stop". Direct evidence that true equilibrium is not attained is simple: ions are observed. Since laser irradiation cannot create net charge from an uncharged sample, recombination of any ions formed, an exoergic process under MALDI conditions, would return the system to an uncharged state, and no mass spectrum would be measurable.

That the kinetics, and well as energetics, of MALDI reactions are important when seeking to achieve quantitative accuracy has been recognized for some time. The only models which have had any success in this direction have been explicitly constructed to include physical and chemical dynamics, before and during the plume expansion [7–9]. This work builds on the rate equation models of 2002 [7] and 2003 [8] to construct a complete model of all ions in a MALDI event, positive and negative, matrix and analyte.

That matrix–analyte reactions may under some circumstances, go far toward local thermal equilibrium in the plume is not in doubt. An investigation of positive and negative ions (separately)

* Tel.: +41 1 632 38 75; fax: +41 1 632 12 92.
E-mail address: rknochenmuss@gmx.net.

1387-3806/$ – see front matter © 2009 Elsevier B.V. All rights reserved.
doi:10.1016/j.ijms.2009.05.002

found clear transitions between kinetically and thermodynamically dominated regimes as a function of laser fluence [10]. Kinsel et al. [11], also found that the logarithm of matrix/analyte ion ratios (in one polarity) was linear vs. reaction free energy, as expected if matrix–analyte ion–molecule reactions approach equilibrium. In general, the thermodynamics of matrix–analyte ion–molecule reactions are highly successful in qualitatively predicting MALDI spectra [6] but until Refs. [1] and [5] it was not suggested that thermodynamics should be sufficient to quantitatively predict ion ratios, and, in particular, PNAIRs.

The bipolar rate equation model presented here shows that the assumption of equilibrium between analyte positive and negative ions is not generally valid, due to kinetic limitations. This is fully consistent with the data. Matrix–analyte reactions in each polarity, however, are often rapid and extensive. The effect on the PNAIR of various experimental variables is also considered, as are suppression effects in one polarity as a function of reactions in the opposite polarity.

2. Methods

The rate equation model used here was closely based on those developed in Refs. [7,8]. In the earlier models, positive and negative ions were assumed to be equal in quantity, which significantly reduced the number of differential equations needed. For the present application, and to make the model more exact, equations for positive and negative ions were explicitly included, but no new physical or chemical phenomena were added. The differential equations may be found in the supplemental material.

The rate equation model for primary ionization in MALDI [7] was developed for the matrix 2,5-dihydroxybenzoic acid (DHB), and those parameters are also used here. The reader is referred to [7] for a full discussion, but in summary matrix ions are created by a two step pooling process. Two matrix molecules in the first excited state (S_1) pool their energy to give one highly excited matrix molecule (S_n state), and a ground state molecule. A molecule in the S_n state can again pool with an S_1 or S_n molecule to concentrate sufficient energy on one molecule to ionize it. Several radiative and non-radiative processes are included, with parameters based on experimental data for DHB.

The sample is assumed to change from the condensed to the gas phase at a fixed temperature (450 K), after which it expands isentropically into the vacuum. Bimolecular reaction rates are scaled by the pressure drop from the time of phase change. The "orifice" from which this molecular beam expands is taken to be the laser spot diameter, 0.1 mm unless otherwise noted. The spot is assumed to be uniformly illuminated by a 355 nm Nd:YAG laser beam, with 5 ns FWHM gaussian temporal profile. Absorption of the laser pulse as it propagates into the bulk is modeled, including stimulated emission, and hence saturation of absorption. The material is divided into thin slices, typically 150, with the thickness varying to keep the absorbed energy per slice constant. The full model is integrated for each slice separately and the results summed. There is negligible mixing or diffusion between slices, since the material expands away from the surface at Mach numbers well above 1, and the first layers are faster than later, deeper layers. The expansion velocity includes a component due to the rapid thermal expansion prior to phase change.

Addition of analyte to the matrix ionization model [8] was achieved by using Arrhenius rates to model the matrix–analyte ion–molecule reactions. Nonlinear free energy relationships provided the necessary activation energies as a function of reaction exoergicity. Protonation/deprotonation reactions were assumed, which is appropriate for a large range of MALDI applications, and these are again assumed here. Excluded volumes and molecular thermal velocities are dependent on analyte molecular weights, here this was always taken to be 1000 Da.

As noted above, the major change necessary to create the model used here was to duplicate all ion differential equations to separately follow positive and negative ion populations. In addition, the recombination equations and terms were extended to explicitly include all combinations of positive and negative ions. Because the previous model treated recombination in a partially parameterized manner, the explicit approach here required a different Arrhenius prefactor to arrive at similar overall rates. The value $1.5 \times 10^9\ s^{-1}$ was used, except where otherwise noted.

Charge and mass balance were checked during the integration, which used double precision, 5th order Runge Kutta methods, with adaptive step size, and a truncation relative error limit of 10^{-8}, in the Igor Pro environment (Wavemetrics, Lake Oswego, USA).

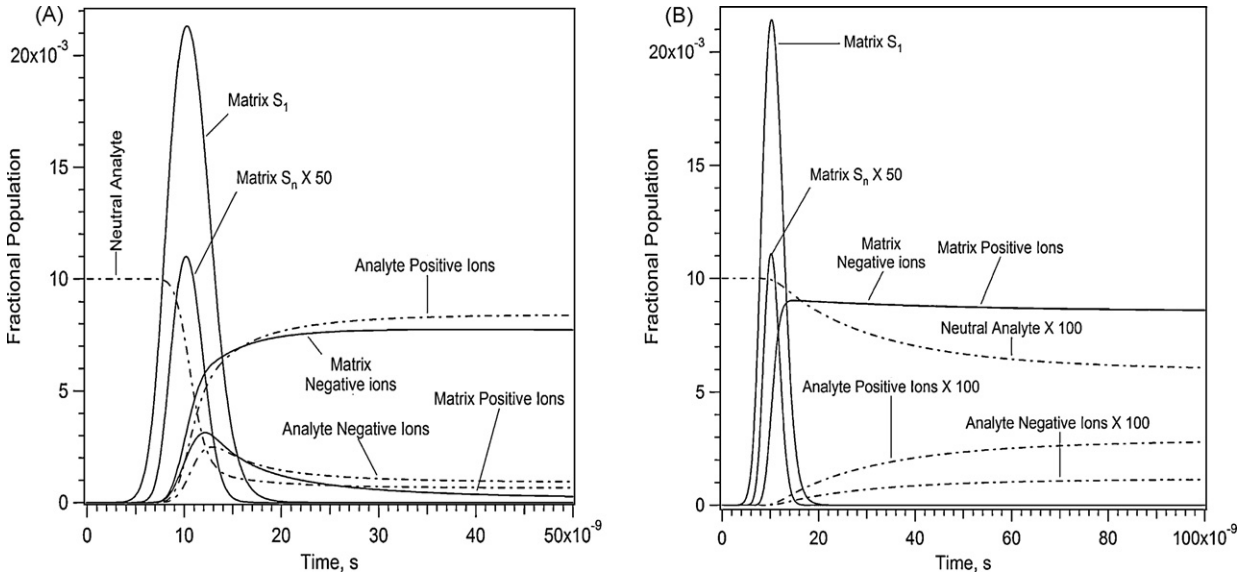

Fig. 1. Time evolution of key species in a MALDI event, as calculated using the rate equation model. Both positive and negative ions are included, of matrix and one analyte. Some important parameters for the calculation were: ΔG for reaction of positive matrix ions with neutral analyte: −60 kJ/mol, ΔG for reaction of negative matrix ions with neutral analyte: −20 kJ/mol, laser fluence: 14 mJ/cm^2. In panel (A) the initial analyte mole fraction is 0.01, in panel (B) it is 0.0001.

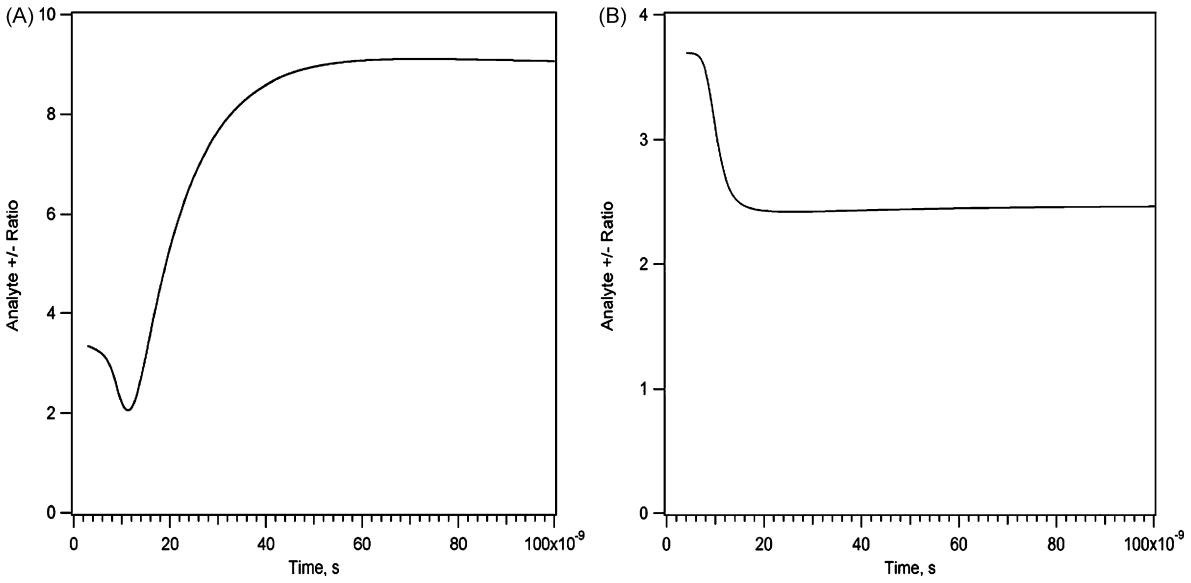

Fig. 2. Time evolution of the positive/negative analyte ion ratio (PNAIR) from the calculations of Fig. 1. matrix–analyte forward reactions proceed quickly, leading to an early imbalance of charge-complementary analyte ions. Slow reverse reactions hinder approach to equilibrium values of the PNAIR. In panel (A) the initial analyte mole fraction is 0.01, in panel (B) it is 0.0001.

3. Results and discussion

3.1. Dynamic vs. static MALDI models of positive/negative analyte ion ratios

An example of the time evolution of the key species in a MALDI event is shown in Fig. 1, for two analyte concentrations spanning an analytically relevant range. As described above, nonlinear processes convert laser energy into primary matrix ion pairs. No net charge is created, overall charge balance is retained at all times. Without ejection of ions into the gas phase, the sample would return to a steady state containing no ions. Fortunately for mass spectrometry, a phase change does occur, which drastically reduces the density of the sample and the rate of bimolecular reactions such as charge transfer and recombination. The density change is also a dynamic event and reactions continue at decreasing rates for a certain time after vaporization. MALDI is an interplay of chemical and physical dynamics which leads to analytically useful ion products.

The rates of MALDI charge transfer processes depend on concentrations of reactants and products, as well as the plume pressure and temperature, and hence are not constant throughout the event. As a result, there is no well-defined initial quantity of matrix ions (as assumed by the static model), and the PNAIR can vary substantially over time, as seen in Fig. 2.

In the examples shown, the reaction of matrix ions with analyte proceeds nearly as fast as matrix ions are created. The more favorable positive reaction is, however, somewhat faster and clearly

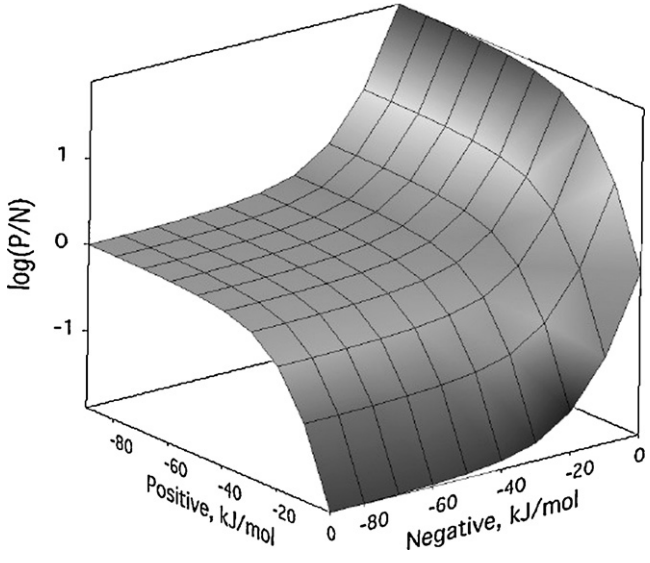

Fig. 3. PNAIR surface as a function of matrix–analyte reaction free energies. The matrix ion generation parameters (pooling rates) were reduced to ensure that matrix ion concentrations remained below the initial analyte mole fraction (0.001) at all times during the calculation. The PNAIR is dominated by a large plateau of equal positive and negative analyte ion concentrations for strongly negative ΔG. Only when one or the other reaction is less favorable ($\Delta G > -30$ kJ/mol) is a significant analyte ion asymmetry predicted.

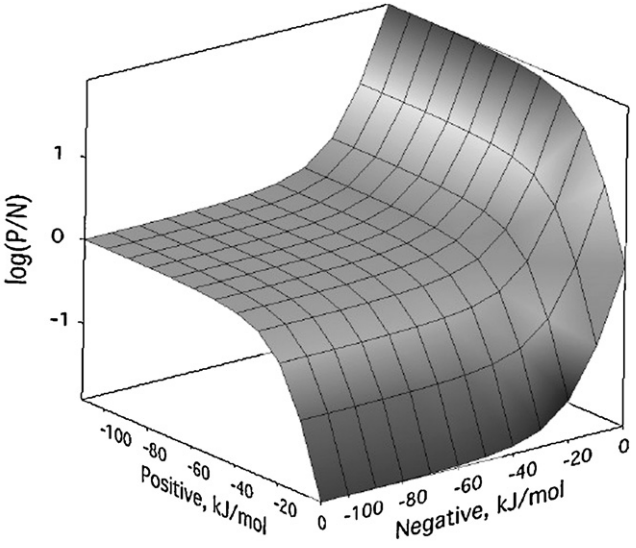

Fig. 4. PNAIR surface as a function of matrix–analyte reaction free energies. The same conditions were used as in Fig. 3, except that matrix ion generation parameters were not artificially reduced. This had the consequence that matrix ion concentrations remained above the initial analyte mole fraction (0.001) at all times during the calculation. Although this represents the inverse limiting case vs. Fig. 3, the PNAIR surface is nearly identical.

more extensive. At early times, the PNAIR is far from equilibrium, which then slowly begins to be established over a time scale several times longer than that of initial ion generation. Analyte positive ions increase at the expense of analyte negative ions, as the compensating inverse shift in matrix ions simultaneously takes place.

For analytical purposes, and for comparison with experiment, only the ion ratios at the right edges of Fig. 2 are relevant (200 ns in the figures below, unless otherwise noted). After extensive plume expansion, the charge transfer and recombination rates become very low due to the low density. At low density ion motion is also no longer dominated by collisions, but by any external electric fields, causing ions to be separated by charge and mass. The long-time ion populations in calculations like that of Fig. 2 are therefore taken here to represent the observable relative intensities in a mass spectrometer.

The final PNAIR in Fig. 2A is 9. This can be compared to the static equilibrium model, with the assumption of 7×10^{-3} initial concentration of positive and negative matrix ions (the peak value for either in Fig. 1A). Solving the coupled equations numerically, to avoid any approximations, leads to a value of 7.7, demonstrating a certain consistency between the approaches in this particular case. As will be seen below, the results are not consistent for other reaction free energies.

There is also the problem in the static approach of choosing the matrix ion initial quantities. Since they are not constant, and not quantitatively predictable without further information, arbitrary choices can result. If, as in Ref. [5], we take a round number like 1×10^{-3} instead of 7×10^{-3}, the static PNAIR is 5.5 about half too low. If 1×10^{-4} is believed to be more appropriate, the result is 16.7, about twice too large. If we take the long-time values from Fig. 1, as more relevant during most of the plume expansion ($M^+ = 1 \times 10^{-3}$ and $M^- = 7 \times 10^{-3}$), the result is 1.2, a factor of 7 incorrect.

Assuming that an initial ratio of matrix ions to neutral analyte can be defined, this ratio was found to determine two major regimes in the static model. If analyte is in excess and the reaction free energies are favorable, charge transfer to analyte may proceed far toward completion, and matrix ions are the limiting reagent in both polarities. The analyte PNAIR will then be very close to 1, since nearly all matrix ions have reacted to form analyte ions, and charge balance must be retained. If reaction in only one polarity is highly favorable, the ratio will deviate from 1, in the obvious direction. This range of behaviors is reflected in Fig. 3, which is dominated by a large plateau region of PNAIR close to 1. (The ion formation parameters were modified to ensure that there was more analyte than matrix primary ions at all times. Note that only negative free energies are plotted, since positive values would lead to negligible analyte ion signal, and are experimentally irrelevant.) In this case, the rate equation model predictions are quite similar to those of the decoupled and coupled mass balance predictions (Ref. [4] Fig. 3, and Ref. [5] Fig. 1).

The results in the case of more matrix primary ions than initial analyte are seen in Fig. 4. Once again, a large plateau is again predicted by the rate equation model, in contrast to the steeply sloping surface predicted by the static coupled equilibrium model (Ref. [5] Fig. 2), but similar to the decoupled model.[4] The similarity between this result and Fig. 3 is remarkable and will be investigated next, but it should first be emphasized that Figs. 3 and 4 represent an important conclusion of this work: a dynamic model of MALDI predicts nearly equal amounts of positive and negative analyte ions over wide ranges of reaction free energies. This is consistent with the 2007 data [1].

Fig. 4 shows that full charge transfer reaction equilibrium is not reached in the plume, in spite of the many collisions and substantial time scale of the expansion. Greater or lesser approach to complete equilibrium can be observed in the dynamic rate equation model in a straightforward manner. Switching off the plume expansion is an

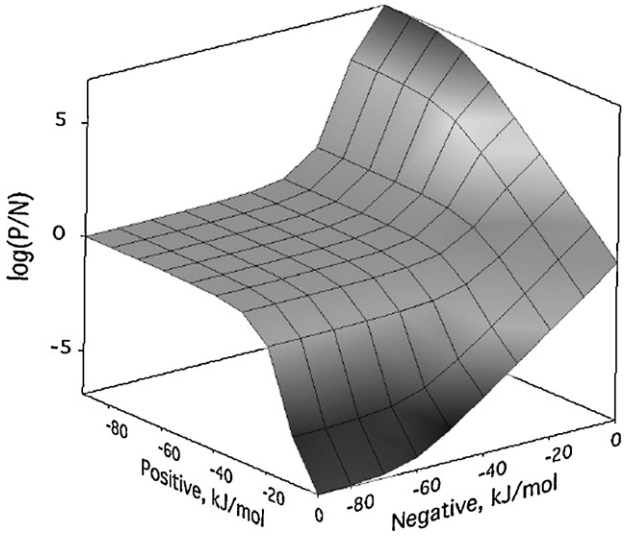

Fig. 5. PNAIR surface as a function of matrix–analyte reaction free energies. The same conditions were used as in Fig. 4, except that plume expansion (which modulates the reaction rates) and recombination were switched off. The integration time was 100 ns.

obvious first step, but this was found to be insufficient. In addition, a major factor neglected in the static approach needs to be considered: recombination as a loss channel. Even without the decrease in rates due to the plume expansion, recombination depletes ion concentrations. As ion concentrations drop, so do charge transfer reaction rates. Recombination is therefore a significant factor in the speed of approach to equilibrium. If both expansion and recombination are switched off, the result of Fig. 5 is obtained.

The inclined plane of Fig. 2 of Ref. [5] begins to appear in the regions where reaction free energies are relatively low, more positive than about −20 to −30 kJ/mol. Nevertheless, a distinct plateau of PNAIR = 1 remains in the central region of more favorable reac-

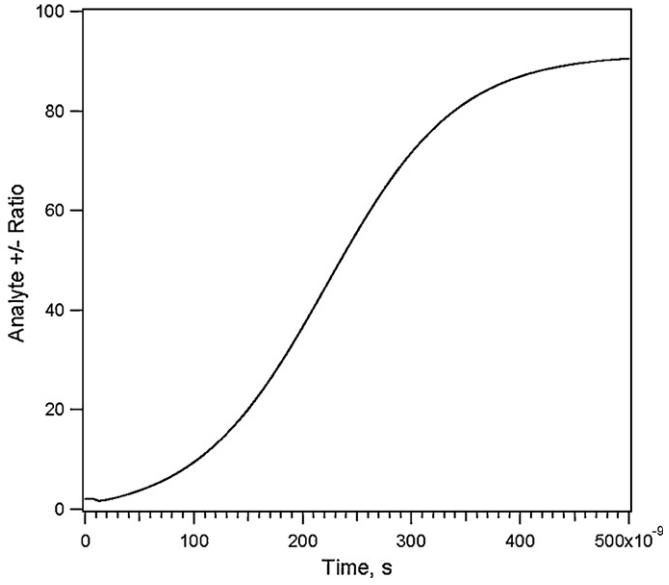

Fig. 6. Time evolution of the PNAIR in a MALDI event, as calculated using the rate equation model. As in Fig. 5, the plume expansion and recombination were switched off. These conditions allow the slow approach to PNAIR equilibrium to be observed in the plume. Some important parameters for the calculation were: ΔG for reaction of positive matrix ions with neutral analyte: −45 kJ/mol, ΔG for reaction of negative matrix ions with neutral analyte: −25 kJ/mol, initial analyte mole fraction: 0.001, laser fluence: 20 mJ/cm^2, laser spot diameter: 0.1 mm.

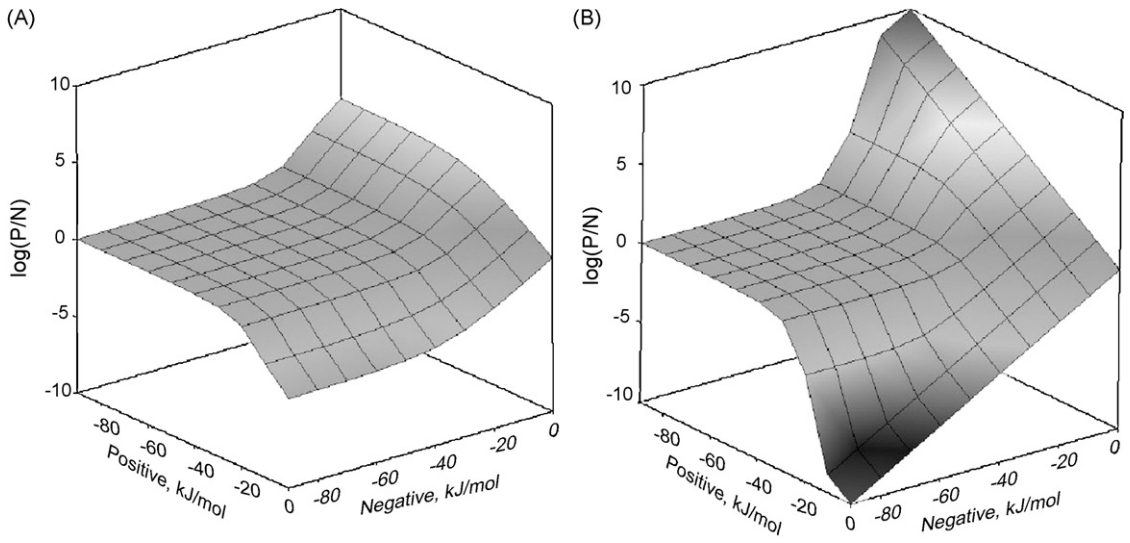

Fig. 7. PNAIR surface as a function of matrix–analyte reaction free energies, for two integration time limits, corresponding to different delayed extraction times. The same conditions were used as in Fig. 4, except that plume expansion and recombination were switched off. In panel (A) the integration time was 50 ns, in (B), 500 ns. The more extensive approach to equilibrium in (B) is apparent from the more pronounced ratios at the edges. Nevertheless, the central plateau remains extensive and flat.

tions. The reasons for this and for the plateau in Fig. 4 are the same: slow approach to PNAIR equilibrium due to fast matrix–analyte forward reactions.

In the plateau region the matrix–analyte driving force is greater than that of the net analyte ion interconversion reaction $A^+ \leftrightarrow A^-$, which is the difference between the two matrix–analyte reaction energies. If the positive matrix–analyte ΔG is −80 kJ/mol, and the negative one is −60 kJ/mol, the positive analyte ions are favored over the negative by only −20 kJ/mol. Reaction to shift analyte from the negative ionic form to the positive form must proceed via regeneration of neutral analyte by reaction with matrix, followed by reaction with matrix negative ions.

In the early MALDI condensed phase and dense plume, neutral A is rapidly depleted by reaction with matrix before it can mediate approach to the equilibrium PNAIR. The reverse matrix–analyte reactions, leading from analyte ions back to analyte neutral are very slow, precisely because the forward reactions are very favorable and fast. The early imbalance in PNAIR is therefore reestablished only slowly compared to the MALDI time scale. This is illustrated in Fig. 6.

The time scale for analyte approach to equilibrium in Fig. 6 is on the order of hundreds of nanoseconds. This is the same time scale as the delayed extraction used in many time of flight mass spectrometers to improve mass resolution. Varying the total time of the numerical integration of the rate equation dynamic model therefore is equivalent to varying the field-free time before extraction. As seen in Fig. 7, the PNAIR surface undergoes some modulation between larger and smaller plateau regions, as the kinetics of the analyte reactions are truncated at different time points. Note, however, that these plots are again with plume expansion and recombination switched off, to emphasize the effect. Realistic modeling of the delayed extraction effect is shown below.

3.2. Parameter dependence of PNAIR in the dynamic reaction model

As noted above, the ratio of initial analyte concentration in the sample and the concentration of primary matrix ions are important determinants of the PNAIR. To aid understanding of the effects to be expected in the laboratory, it is useful to consider some examples where one parameter is varied while others are held constant.

If a moderate laser fluence is chosen (5 mJ/cm^2 above the threshold) variation of analyte concentration over 3 orders of magnitude

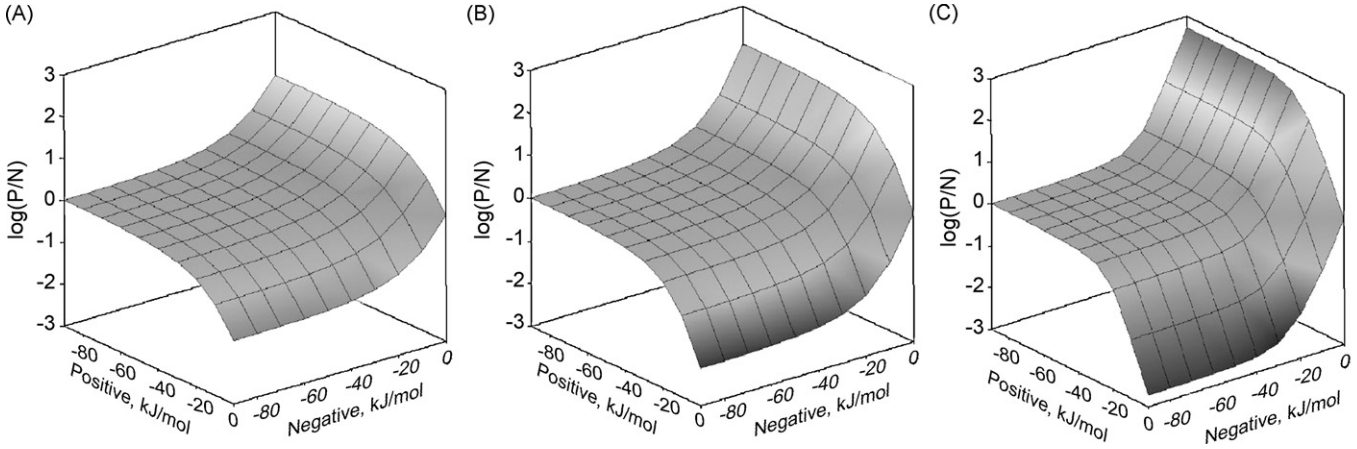

Fig. 8. PNAIR surface as a function of matrix–analyte reaction free energies, and at three analyte mole fractions: 0.0001 in (A), 0.001 in (B), and 0.01 in (C). The laser fluence was 17 mJ/cm^2. Normal parameters were used, including plume expansion and recombination. Approach to PNAIR equilibrium is faster at higher analyte mole fractions, but the plateau is present in every case.

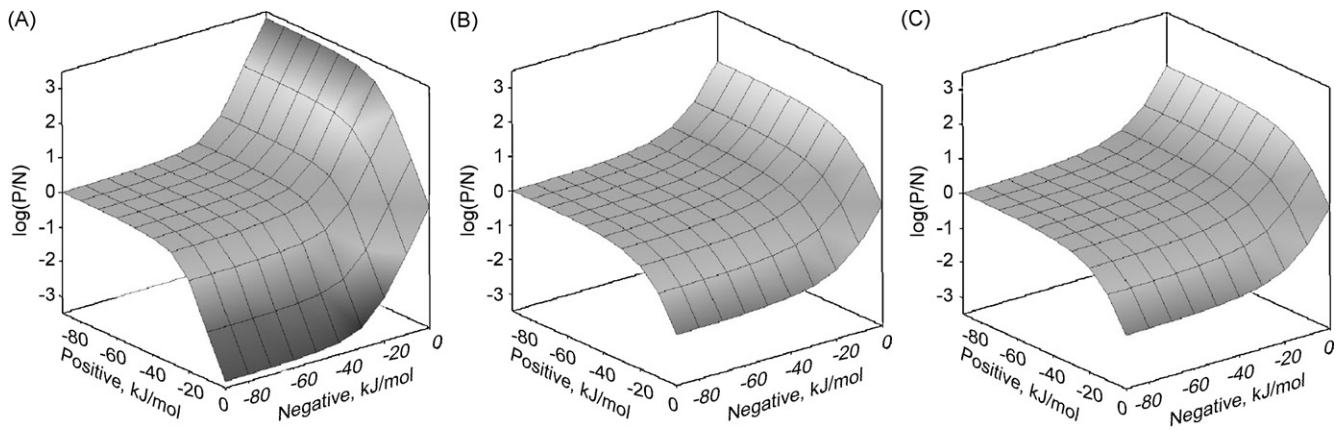

Fig. 9. PNAIR surface as a function of matrix–analyte reaction free energies, and at three laser fluences: 12 mJ/cm^2 in (A), 17 mJ/cm^2 in (B), and 22 mJ/cm^2 in (C). The analyte mole fraction was 0.001. Normal parameters were used, including plume expansion and recombination. Approach to PNAIR equilibrium is more extensive at lower fluences due to longer reaction times before plume dilution, but the plateau is present in every case.

leads to the PNAIR surfaces of Fig. 8. These calculations were carried out with the standard model parameters believed to represent a typical MALDI event, including plume expansion and recombination.

At 10^{-4} analyte concentration, not atypical for many MALDI experiments, the PNAIR surface is quite flat. This is a reflection of the fact that reaction rates are proportional to concentrations, so approach to LTE is slow. The highest concentration shown in Fig. 8, 1%, is not often used in MALDI unless it is desired to enhance analyte/matrix ion ratios via the matrix suppression effect. This is usually only needed for low molecular weight analytes, to reduce spectral congestion from matrix. The higher reaction rates are evident in more pronounced extrema at the edges of the surface. At the same time, the plateau region of PNAIR near 1 is not noticeably smaller than for the lowest concentration.

Variation of fluence at a reasonably typical analyte concentration of 0.001 leads to the PNAIR surfaces of Fig. 9. Lower fluence has the consequence that the sample takes longer to reach the phase change temperature, so approach to LTE can be more extensive before plume expansion quickly reduces the reaction rates. After the fluence is more than slightly above threshold, the PNAIR surfaces are rather flat, and do not change substantially with increasing fluence. Most MALDI experiments use fluences comfortably above threshold to arrive at a useful compromise between intensity and resolution, so panels B or C of Fig. 9 are likely to represent typical results.

Diode-pumped, frequency tripled Nd:YAG lasers seem to have become the preferred excitation source in MALDI instruments, but many nitrogen discharge lasers are still used, emitting at 337 nm. This wavelength is better absorbed by some matrixes than 355 nm, and the photon energy is higher. These factors result in greater thermal energy deposition in the top sample layers, leading to a lower ablation fluence threshold [7]. Since the user will adapt the fluence as noted above, the resulting plume expansion characteristics are not strongly dependent on laser wavelength. This is illustrated in Fig. 10, showing PNAIRs for 337 nm excitation (absorption cross section 7 times greater than at 355 nm), at concentrations corresponding to Fig. 8. The surfaces are very similar in the two figures.

As shown above, if recombination and the plume expansion are not included in the model, analyte ions approach LTE on a time scale of hundreds of nanoseconds. The question remains whether variation of the delayed extraction time could be used in practice to vary the PNAIR. Fig. 11 shows calculations using the full model, for reaction times until extraction of 50 and 500 ns. A rather low laser fluence was used, to delay plume formation and increase reaction time. Nevertheless, only very minimal differences are seen between the two surfaces. The 500 ns PNAIR extrema are slightly more pronounced, but these differences probably are not useful, or even observable, in the laboratory.

The laser spot size on the sample is also a factor influencing the rate of plume expansion [12,13], and hence the rates of reaction.

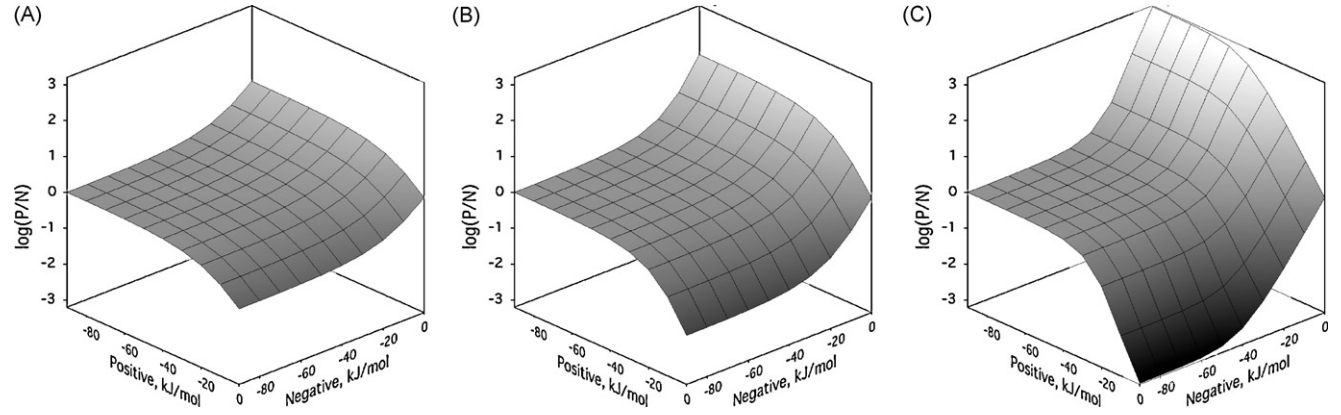

Fig. 10. PNAIR surface as a function of matrix–analyte reaction free energies, and at three analyte mole fractions: 0.0001 in (A), 0.001 in (B), and 0.01 in (C). The laser wavelength was 337 nm, and the fluence was 9 mJ/cm^2, comfortably above the ablation threshold. At this wavelength the matrix absorption cross section was taken to be 7 times greater than at 355 nm. The surfaces are very similar to those of Fig. 8, for 355 nm.

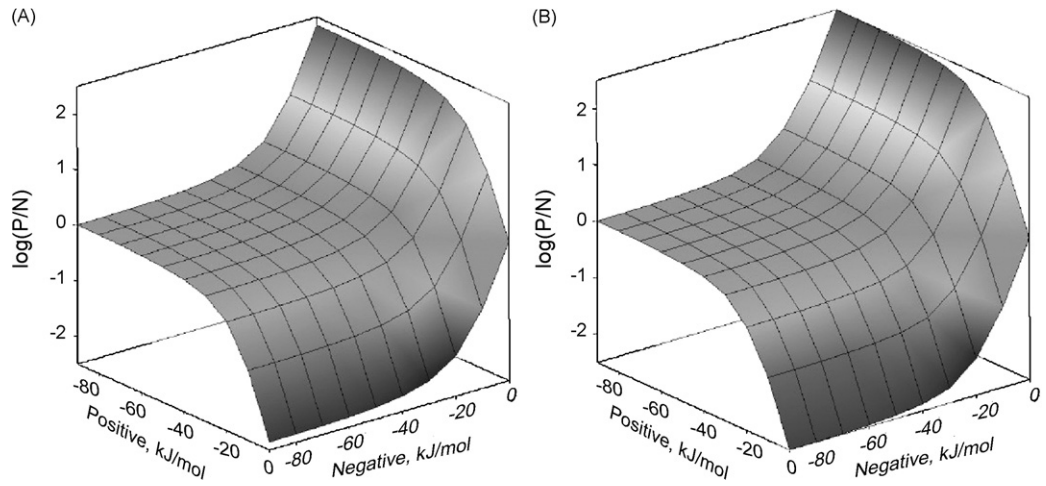

Fig. 11. PNAIR surfaces as a function of matrix–analyte reaction free energies, and at two delayed extraction times: 50 ns in (A), and 500 ns in (B). The analyte mole fraction was 0.001 and the laser fluence 14 mJ/cm^2. Normal parameters were used, including plume expansion and recombination. There is little effect due to extraction delay.

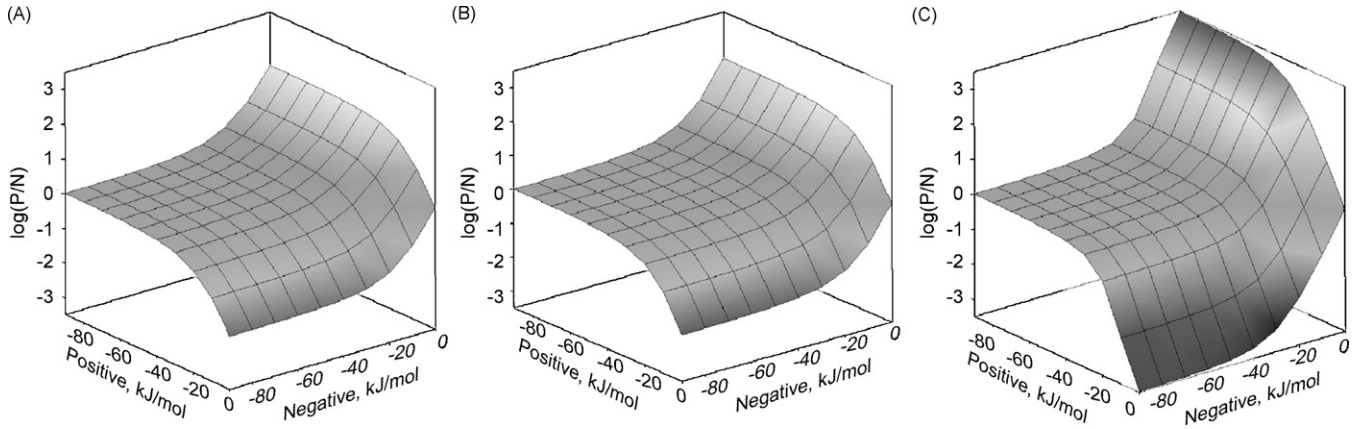

Fig. 12. PNAIR surface as a function of matrix–analyte reaction free energies, and three laser spot diameters: 0.01 mm in (A), 0.1 mm in (B), and 1 mm in (C). The analyte mole fraction was 0.001 and the laser fluence 17 mJ/cm^2. Normal parameters were used, including plume expansion and recombination. Only for atypically large spots (and associated high pulse energies) is there a noticeable increase in approach to PNAIR for less favorable ΔG.

As was previously shown, this leads to nonlinearly varying MALDI yields [7]. The effect on the PNAIR is shown in Fig. 12.

Since smaller spots lead to faster radial and overall expansion, it is expected that they will lead to flat PNAIR surfaces, as seen in Fig. 12, panel A. The spot diameter of panel A, 0.01 mm, is rather tightly focused, probably more so than in most MALDI experiments. Panel B shows a more typical value, 0.1 mm, but the surface is only slightly less flat. Only when the laser spot is made very large (and the pulse energy quadratically increased to maintain the same fluence), does the PNAIR become significantly less flat. The plateau region, however, remains largely unaffected. These calculations suggest that typical MALDI experiments will not observe a significant modulation of the PNAIR due to normal minor variation of the laser spot size.

3.3. The dynamic reaction model and suppression effects

3.3.1. Matrix suppression effect

Suppression of matrix ions by analyte is a straightforward consequence of secondary plume reactions (matrix suppression effect, MSE). If sufficient analyte is present, matrix ions are the limiting reagent. When the forward matrix–analyte reaction is kinetically and thermodynamically favorable, matrix ions can be depleted to a negligible level. MSE has been observed in both polarities [2,3]. Since analyte rather than matrix ions are the desired result, this

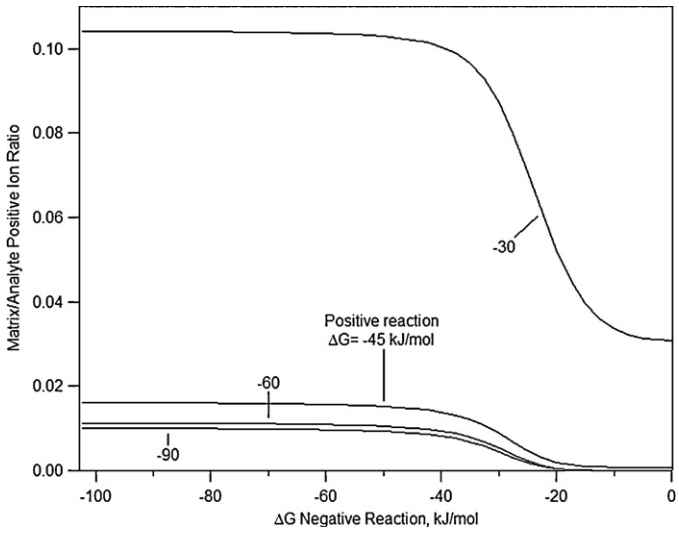

Fig. 13. Matrix/analyte ion ratio in positive mode, as a function of negative ion secondary reaction ΔG, and for positive ion secondary reaction ΔG values ranging from −30 to −90 kJ/mol. Efficient negative ion reaction depletes neutral analyte, reducing depletion of matrix ions in positive polarity. The MSE is therefore most effective when secondary reactions in the opposite polarity are unfavorable. The analyte mole fraction was 0.02; laser fluence 15 mJ/cm^2 and reaction time 200 ns.

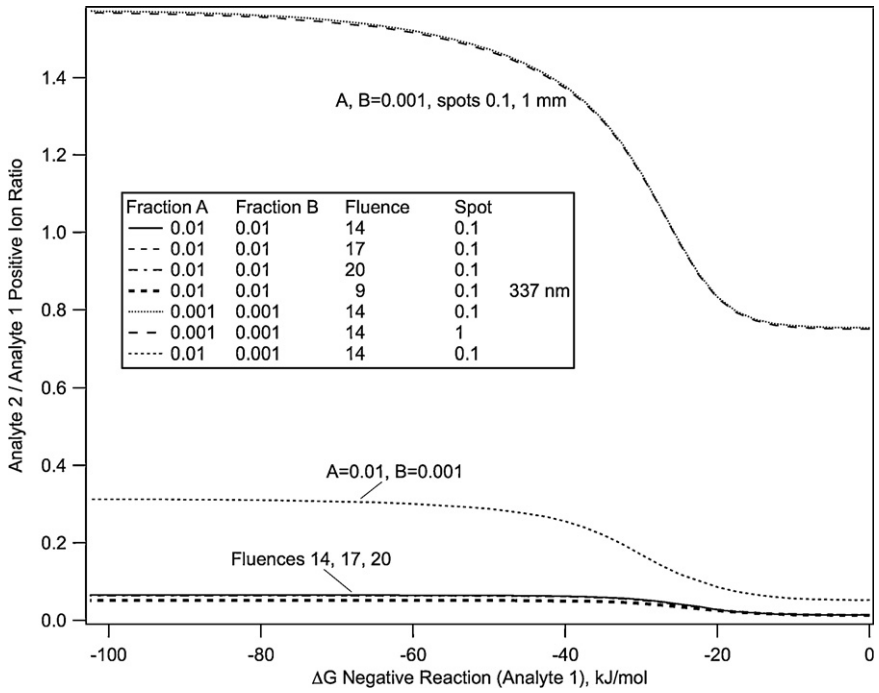

Fig. 14. Ion ratio of two analytes, in positive mode, as a function of negative ion secondary reaction ΔG for analyte 1, and several other parameters. Efficient negative ion reaction depletes neutral analyte, reducing the ion ratio in positive polarity. The ASE is therefore most effective when secondary reactions in the opposite polarity are unfavorable. The positive secondary reaction ΔG for analyte 1 was −100 kJ/mol. The positive secondary reaction ΔG for analyte 2 was −30 kJ/mol, and the negative reaction ΔG −10 kJ/mol. The laser wavelength was 355 nm, except as indicated. The spot diameters are in mm, and the fluences in mJ/cm^2.

can be a useful technique for analysis of low molecular weight analytes [14]. The MSE can be modeled using unipolar rate equations, and the results are in good agreement with experiment [7]. The MSE depends on analyte concentration, secondary reaction free energies (reaction rate and extent), laser fluence (supply of primary matrix ions) and laser spot size (rate of plume expansion).

A factor not previously considered in connection with the MSE is the consumption of analyte neutrals by secondary reactions in the polarity opposite to that in which MSE is desired or observed. If this is extensive, there may not be enough analyte remaining to achieve full MSE. Equivalently, a higher analyte concentration is required for MSE if reactions in both polarities are efficient, compared to the concentration needed if only one reaction is favorable. This cross-polarity effect is demonstrated in Fig. 13.

Better suppression of positive matrix ions (M/A approaching zero) is observed for weak negative ion reactions in this example. As the negative reactions become more favorable, positive mode suppression decreases. The inflection point of the sigmoidal curve is a function of the reaction kinetics, which here are derived from the reaction free energies, as described above. Both positive and negative reactions are taken to have the same free energy dependence, which may not be the case for all analytes.

As noted in Ref. [5], there seems to be some consensus that MSE is more common and stronger in positive than negative polarity. While negative ion thermodynamic data are currently insufficient to draw clear conclusions, it is possible that cross-polarity inhibition of MSE as in Fig. 13 is involved. Hillenkamp et al have recently suggested that negative ion proton transfer reactions $(M{-}H)^- + A \rightarrow M + (A{-}H)^-$ of some peptides with common matrixes may exhibit ΔG values not far from zero [5]. The corresponding positive ion proton transfer reactions, $MH^+ + A \rightarrow M + AH^+$, are generally quite favorable, with ΔG in the range of −100 to −150 kJ/mol. Fig. 13 shows that this combination of reaction energetics would make negative ion MSE difficult.

3.3.2. Analyte suppression effect

A similar cross-polarity effect is predicted to occur for suppression of one analyte by another. Analytes which react favorably with matrix can reduce signal from those with less favorable reaction energetics, in the same polarity (analyte suppression effect (ASE) [3]). As seen in Fig. 14, the efficiency of secondary reactions in the opposite polarity modulates the analyte ion ratios by depletion of neutral populations.

4. Conclusions

The rate equation model for MALDI primary and secondary ionization was extended to explicitly include all ions of both polarities. The model was used to investigate the ratios of positive to negative analyte ions formed by secondary reactions with primary matrix ions, as a function of several parameters. This ratio is found to be near 1, so long as the positive and negative reaction free energies are more than slightly favorable (more negative than about −30 kJ/mol). This is consistent with the experimental data [1].

Also consistent with earlier work, the degree of approach to local thermal equilibrium in the MALDI plume is found to be not only a function of the reaction free energies, but also of the reaction kinetics. Full equilibrium among all ion species cannot be assumed for quantitative prediction or analysis of MALDI results.

The deviation of charge-complementary analyte ion populations from equilibrium is most pronounced when the reactions of primary matrix ions with neutral analyte are significantly exoergic in both polarities. The forward reactions are then fast, and non-equilibrium populations of analyte ions of opposite polarity are thereby generated. Since the forward reactions are fast, the reverse reactions are slow, and equilibration of oppositely charged analyte ions cannot take place on the MALDI time scale. The polarities remain largely decoupled.

Factors influencing the PNAIR for a given analyte are laser fluence, concentration, spot size, and extraction delay. These factors need to be controlled in any future experiments investigating PNAIR surfaces, even though the effects are mostly weak. They may be understood based on considerations of reaction rates and extent before plume dilution. In all cases, the PNAIR is predicted to be near unity in a central plateau region where reactions in both polarities are significantly exoergic.

Rapidly varying PNAIR surfaces are expected only due to reaction kinetics which have much different dependence on reaction energetics than embodied in the free energy relationships used here. If forward matrix–analyte reactions were much slower and/or reverse reactions much faster, in one or both polarities, the surfaces might not be so flat. Investigation of MALDI phenomena therefore should not loose sight of possible kinetic effects, simply because thermodynamics often is a major factor.

The bipolar model was also used to investigate suppression effects in MALDI. Depletion of neutral analyte by efficient opposite-polarity reactions reduces ion ratios in a straightforward manner. The relative magnitudes of the reaction free energies, and hence the reaction kinetics, in the two polarities can especially influence matrix/analyte ion ratios. This may explain qualitative observations regarding relative signal strength in positive vs. negative polarities for some analyte classes like peptides.

Appendix A. Supplementary data

Supplementary data associated with this article can be found, in the online version, at doi:10.1016/j.ijms.2009.05.002.

References

[1] M. Dashtiev, E. Wäfler, U. Röhling, M. Gorshkov, F. Hillenkamp, R. Zenobi, Int. J. Mass Spectrom. 268 (2007) 122.
[2] R. Knochenmuss, F. Dubois, M.J. Dale, R. Zenobi, Rapid Commun. Mass Spectrom. 10 (1996) 871.
[3] R. Knochenmuss, V. Karbach, U. Wiesli, K. Breuker, R. Zenobi, Rapid Commun. Mass Spectrom. 12 (1998) 529.
[4] R. Knochenmuss, Int. J. Mass Spectrom. 273 (2008) 84.
[5] F. Hillenkamp, E. Wäfler, M.C. Jecklin, R. Zenobi, Int. J. Mass Spectrom. 285 (2009) 114.
[6] R. Knochenmuss, Analyst 131 (2006) 966.
[7] R. Knochenmuss, J. Mass Spectrom. 37 (2002) 867.
[8] R. Knochenmuss, Anal. Chem. 75 (2003) 2199.
[9] R. Knochenmuss, L.V. Zhigilei, J. Phys. Chem. B 109 (2005) 22947.
[10] K. Breuker, R. Knochenmuss, J. Zhang, A. Stortelder, R. Zenobi, Int. J. Mass Spectrom. 226 (2003) 211.
[11] G.R. Kinsel, D. Yao, F.H. Yassin, D.S. Marynick, Eur. J. Mass Spectrom. 12 (2006) 359.
[12] K. Dreisewerd, M. Schürenberg, M. Karas, F. Hillenkamp, Int. J. Mass Spectrom. Ion Proc. 141 (1995) 127.
[13] D. Feldhaus, C. Menzel, S. Berkenkamp, F. Hillenkamp, J. Mass Spectrom. 35 (2000) 1320.
[14] G. McCombie, R. Knochenmuss, Anal. Chem. 76 (2005) 4990.